

Interface controlled electronic variations in correlated heterostructures

K. Gehrke,¹ V. Moshnyaga,¹ K. Samwer,¹ O. I. Lebedev,² D. Kirilenko,² and G. Van Tendeloo²

¹*I. Physikalisches Institut, Georg-August-Universität Göttingen,
Friedrich-Hund-Platz 1, 37077 Göttingen, Germany*

²*EMAT, University of Antwerp, Groenenborgerlaan 171, B-2020 Antwerpen, Belgium*

An interface modification of (LaCa)MnO₃ – BaTiO₃ superlattices was found to massively influence magnetic and magnetotransport properties. Moreover it determines the crystal structure of the manganite layers, changing it from orthorhombic (Pnma) for the conventional superlattice (cSL), to rhombohedral (R3c) for the modified one (mSL). While the cSL shows extremely nonlinear ac transport, the mSL is an electrically homogeneous material. The observations go beyond an oversimplified picture of dead interface layers and evidence the importance of electronic correlations at perovskite interfaces.

Interfaces of complex oxides have gained much attention since the discovery of a high-mobility quasi two dimensional electron gas at the TiO₂/LaO-interface between insulating LaAlO₃ (LAO) and SrTiO₃ (STO) [1, 2]. This unexpected finding disclosed a new role of interfaces in oxide heterostructures. Thereby the reconstruction of the interface is discussed to avoid an electrostatic potential, otherwise building up in the lanthanum perovskite. For this reconstruction either electrons redistribute or ions rearrange through relaxation or deviation from stoichiometry. The charge transfer can effectively dope the materials in a rather thin region in the vicinity of the interface [3, 4], and the resulting change in carrier concentration due to the presence of an interface can be termed “interface doping”. For strongly correlated electron systems it is well known that the carrier concentration massively influences the properties of the material. A prominent example is the class of perovskite manganites, which are interesting not only because of high spin polarization in the ferromagnetic phase [5, 6], but also due to the fascinating rich magnetic phase diagram that opens up upon doping [7]. The ground state of La_{1-x}Ca_xMnO₃ (LCMO) changes from ferromagnetic (FM) metallic for $0.2 \leq x \leq 0.4$ to antiferromagnetic (AFM) insulating for $x \geq 0.5$, whereas the phase boundary is not a sharp line, but rather a broad region around $x = 0.45$ where FM and AFM phases coexist [8]. The FM state is stabilized by gaining kinetic energy due to the delocalization of charge carriers at the expense of antiferromagnetic exchange of localized spins. Localization is stabilized by the Jahn-Teller (JT) effect, that lifts the e_g-orbital degeneracy of Mn³⁺ ions [9], giving rise to JT-polarons, that are discussed to be the main type of charge carrier at all temperatures [10]. Binding of these JT-polarons into pairs of correlated polarons (CP) or bipolarons is now argued to bring about the strong localization at the metal insulator (MI) transition [11]. Even for optimal doping ($0.2 \leq x \leq 0.4$) correlated JT polarons have been observed by neutron and x-ray scattering [12, 13], with the wave vector of these short range JT-distorted regions being $\vec{q} = [\frac{1}{4}, \frac{1}{4}, 0]$.

The loss of FM order in La_{2/3}Ca_{1/3}MnO₃ (LCMO) and La_{2/3}Sr_{1/3}MnO₃ (LSMO) below a critical film thickness

[14, 15], and the poor performance of LSMO-STO-LSMO tunnel junctions at elevated temperatures [16, 17], have been connected to the weakening of double exchange at manganite interfaces. The breakup of the Mn-O chains has been accounted for this interface-induced phase separation [18] and the carrier depletion (interface doping), alike the one discussed for LAO/STO-interfaces, seems to be a driving force of the localization. Moreover it has been shown that two monolayers of LaMnO₃ (LMO) introduce extra carriers to the interface region, counteracting the depletion and stabilizing the FM/spin polarization [16, 17, 19]. Elastic constraints also play an important role, since lattice relaxations are intrinsically coupled to the electronic correlations in Jahn-Teller Systems [20]. Furthermore CP can be attributed to the CE-AFM phase, which shows the same superstructure wave vector $\vec{q} = [\frac{1}{4}, \frac{1}{4}, 0]$. As we have shown recently, CP can be probed by means of the 3rd harmonic voltage, which is a measure of electric nonlinearity, because of their quadrupole nature [21]. Here we use AC-transport, SQUID magnetometry and transmission electron microscopy (TEM) to study the influence of interfaces in SLs and the effect of an interface modification by additional LMO layers.

We compare the physical properties of two manganite-titanate superlattices (SL). The conventional SL (cSL) consists of 40 unit cells (u.c.) LCMO and 20 u.c. BaTiO₃ (BTO), repeated ten times [LCMO₄₀/BTO₂₀]₁₀. The modified SL (mSL) consists of the same LCMO and BTO layers, but additionally two u.c. of LMO were introduced at each interface: [LCMO₄₀/LMO₂/BTO₂₀/LMO₂]₁₀. The SLs were grown on MgO (100) substrates at $T = 900^\circ\text{C}$ by means of a metal organic aerosol deposition technique [22]. The mono-layer accuracy during deposition was achieved by controlling the volume of the metal organic solution for each layer.

The XRD (Θ - 2Θ) patterns show typical satellite peaks, arising from the SL periodicity (not shown). The calculated periodicities from Schuller’s formula [23] are $\lambda_{cSL} = 23.3 \pm 0.05 \text{ nm}$ and $\lambda_{mSL} = 25.3 \pm 0.05 \text{ nm}$, which is in a good agreement with the nominal thicknesses. A detailed study of the crystal and chemical structure of SLs was performed on cross-section and plan view spec-

imens by means of TEM. Plan view and cross section electron diffraction (ED) (Fig.1a,b) patterns clearly show heteroepitaxial growth of all layers for both SLs. Cross-section high resolution TEM (HRTEM) images confirm epitaxial growth of SLs and show coherent, atomically flat and sharp interfaces (Fig.1c,d). The extra LMO layers in mSL are not visible in HRTEM image but, obviously, introduce significant structural differences between cSL and mSL as it can be detected by ED and HRTEM. The LCMO layer of the mSL exhibits the unusual $R\bar{3}c$ structure in contrast to most bulk samples [24] and cSL LCMO showing both $Pnma$ structure. The structure of BTO of both SLs is found to be close to $P4mm$. The tetragonality of the BTO-layers is $\frac{c}{a} = 1.04 \pm 0.005$ for the conventional and $\frac{c}{a} = 1.025 \pm 0.005$ for the modified SL. Energy filtered TEM (EFTEM) and electron energy loss spectroscopy (EELS) measurements of SLs (not shown) show well defined chemical separation of LCMO and BTO layers leading to the conclusion that there is no large interdiffusion and the interfaces are chemically sharp. In order to analyze strain fields, the geometrical phase analysis (GPA) method [25] has been applied to HRTEM images of cSL and mSL. The results of GPA along the growth direction are shown in Fig.1(e), (f) and reveal inhomogeneously strained cSL, in contrast to the mSL heterostructure which looks homogeneously strained.

Magnetic properties of the SLs have been measured with external field applied parallel to the film plane. The temperature dependence of the magnetization of both SLs, see Fig.2(a) shows a rather broad ferromagnetic transition, typical for thin LCMO-layers [26, 27]. The magnetic Curie temperatures of the SLs are $T_C^{cSL} = 245 K$ and $T_C^{mSL} = 253 K$. Magnetic hysteresis $M(H)$, shown in Fig.2(b) was measured at $T=10K$ after cooling without (zfc) and with an external field $\mu_0 H = 5 T$ applied during cooling (fc). The saturation magnetization (M_s) of the SLs after fc is as large as $M_s^{cSL} = 287 \frac{emu}{cm^3}$ and $M_s^{mSL} = 393 \frac{emu}{cm^3}$, which is smaller than the bulk value, $M_s^{bulk} \approx 650 \frac{emu}{cm^3}$. In the case of the mSL, additional LMO layers are expected to contribute to the magnetic moment and therefore the volumes of both LCMO and LMO were considered calculating M_s^{mSL} . The corresponding coercivities are $H_c^{cSL} = 721 Oe$ and $H_c^{mSL} = 536 Oe$. Interestingly, after zfc the M_s of both SLs were smaller than M_s after fc, $\frac{\Delta M_s}{M_s} \approx -11\%$ for the cSL and $\frac{\Delta M_s}{M_s} \approx -3\%$ for the mSL.

Measurements of the ac electric transport were performed by means of four probe method, with silver paste contacts at the edges of the SLs. The ac-current amplitude was $I_{ac} = 10 \mu A$ and the frequency $f_{ac} = 17 Hz$. Besides the linear electric response with resistance R_ω at the fundamental frequency f_{ac} , we report the third harmonic response at $f_{3\omega} = 3f_{ac}$ in terms of the coefficient $K_{3\omega} = \frac{U_{3\omega}}{U_\omega}$, which is a measure of the electrical nonlinearity in the film [21]. Fig.3(a) shows the temperature dependence of R_ω , measured after field cooling (fc) and

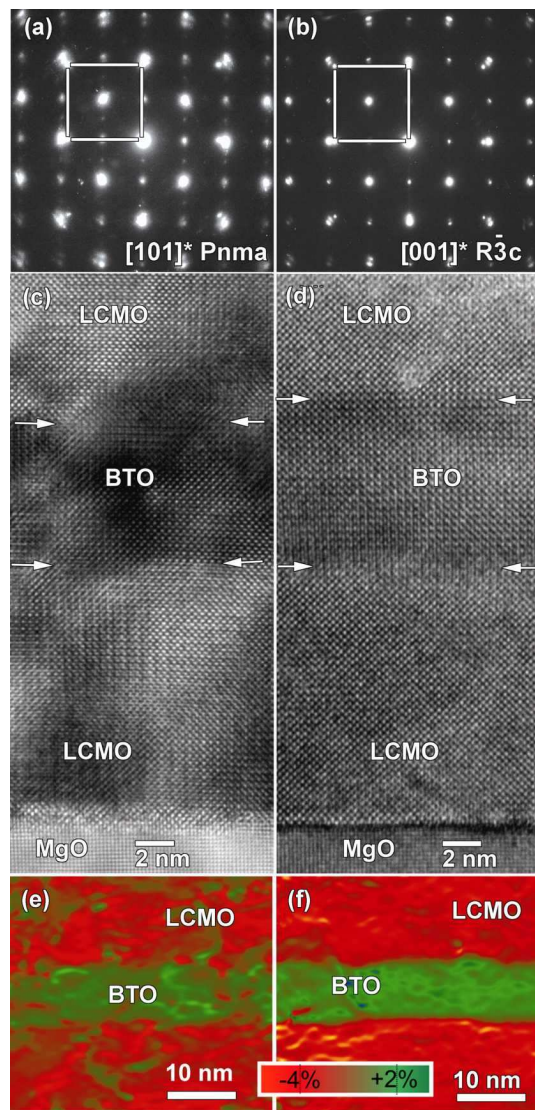


Figure 1: Microstructure analysis of the cSL (left) and mSL (right). Electron diffraction patterns (top) reveal $Pnma$ -symmetry for cSL (a) and $R\bar{3}c$ -symmetry for mSL (b). Cross-section HRTEM (mid) confirm epitaxial growth and coherent interfaces of cSL and mSL (d). GPA (bottom) shows strain fields along the growth direction to be inhomogeneous for cSL (e) and homogeneous for mSL (f)

zero field cooling (zfc). The cSL shows a large difference (factor of ten) between fc and zfc resistance at low temperature, $T = 10 K$. The difference gets smaller at $T \approx 150 K$ and vanishes completely close to $T_c = 245 K$. The metal-insulator (MI) transition of the cSL is shifted by $\Delta T = 77 K$ below the magnetic transition. For the mSL no difference between $R_\omega^{mSL}(fc)$ and $R_\omega^{mSL}(zfc)$ was observed, and $T_c^{mSL} - T_{MI}^{mSL} = 22 K$. Regarding nonlinear transport, shown in Fig.3(b), the cSL shows a strong increase of $K_{3\omega}$ by decreasing temperature, both for fc- and zfc-condition. Two features in $K_{3\omega}(T)$ are distinguishable: at $T = 100 K$ and $T = 255 K$ there exist kinks. Below $T = 100 K$ the non linearity is very

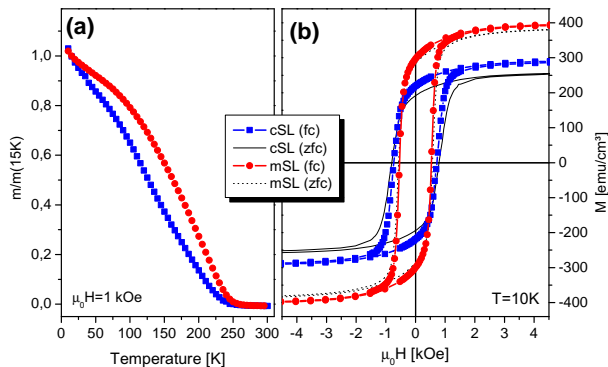


Figure 2: (a) Normalized magnetization as a function of temperature of conventional (cSL) and modified (mSL) superlattice samples. (b) Magnetic Hysteresis of cSL and mSL at $T = 10$ K. Measurements taken after field cooling (fc) and zero field cooling (zfc) are shown.

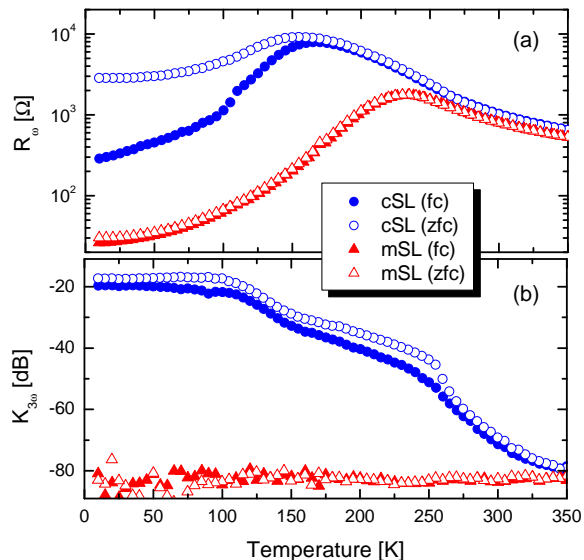


Figure 3: Transport properties of the conventional (cSL) and modified (mSL) superlattice as a function of temperature. Linear ac-resistance R_ω (a) and the nonlinear coefficient $K_{3\omega}$ (b) are shown for field cooled (fc) and zero field cooled (zfc) measurements.

large, $K_{3\omega} \approx -20$ dB, and nearly constant. For the mSL a very small nonlinear signal ($K_{3\omega} < -80$ dB) was measured in the whole temperature range, both for fc- and zfc-condition.

In the case of manganite-titanate interfaces, the concept of interface doping leads to an overall increase of the Mn-valence, which would be equal to an increase of doping to $x = x_{nominal} + x_{interface}$. Recent theoretical and experimental studies show that the length scale on which charge transfer takes place is rather small, $l_{ct} \approx 1$ nm [28, 29], and therefore x is increased only in the vicinity

of the interfaces. By adding LMO-layers we decrease $x_{nominal}$ in this region. The overall doping level at the interfaces of the mSL is smaller compared to that at the cSL interfaces. In this sense, the interface regions bring about different electronic constraints to the LCMO-layers in the SLs. Because of the strong electronic correlations these electronic constraints have tremendous impact on the structural properties of the LCMO-layers.

First of all the enhanced saturation magnetization M_s and reduced coercivity H_c in mSL, see Fig.2(a), directly show that the interface modification strongly reduces the tendency towards AFM correlation. The difference in M_s after fc/zfc and the extreme difference between T_C and T_{MI} for the cSL underlines a pronounced magnetic inhomogeneity of the cSL. Due to the modification magnetic inhomogeneity is reduced in the mSL, which can also be seen in a somewhat steeper magnetic transition (see Fig.2(b)). The difference of the magnetic homogeneity is also reflected by the electric transport behavior of the SLs. The fc/zfc-difference, observed only for the cSL (see Fig.3(a)), can be attributed to an inhomogeneous electronic (phase separated) state, which is known from $La_{1-x}Ca_xMnO_3$ with $0.4 \leq x \leq 0.5$.

Most interestingly, the different electric constraints of the SLs not only change the magnetic and transport properties, but also the structure of the interface region and hence of the whole LCMO-layers. For LCMO without oxygen deficiency, it was shown that crystalline structure, determined by the amount of Mn^{4+} -ions, changes from $R\bar{3}c$ for $x \leq 0.4$ to $Pnma$ for $x \geq 0.5$ [30]. The right oxygenation can be expected in the case of metal organic aerosol deposition technique, as films are grown at ambient oxygen pressure. The manganite of the mSL shows $R\bar{3}c$ symmetry, which has been observed for small amounts of Mn^{4+} -Ions, i.e. $x \leq 0.4$. The LCMO-layers of the cSL show $Pnma$ -symmetry, which is found for $x \geq 0.5$. So, most probably the interface region of cSL is in the CE-AFM state, as it is found for LCMO with $x \geq 0.5$. As we have shown previously [21] the manganites with $R\bar{3}c$ structure (LSMO) show linear transport behavior, whereas for the $Pnma$ structure non linearity has been observed in the transition region. Here we see another example of this rule: the mSL ($R\bar{3}c$) shows a very small $K_{3\omega} \approx -80$ dB, whereas the cSL ($Pnma$) shows pronounced nonlinear transport properties, see Fig.3(b). The extremely large nonlinear signal, $K_{3\omega} > -20$ dB, at low temperatures on the other hand is in contrast to the results for single LCMO-films [21]. This can be attributed to the high density of interfaces of the cSL compared to a single LCMO-film. The interfaces act like nucleation centers, at which the CP can accumulate and therefore the amount of CP is enhanced in cSL. If one assumes the CP to be the building blocks of the CE phase, it is clear that the interface region is unstable against the antiferromagnetic CE-correlations [19]. For the mSL the number of CP is reduced, so that $K_{3\omega}$ is very small. Furthermore the $Pnma$ -symmetry, in contrast to the homogeneous $R\bar{3}c$ -symmetry, allows for local elastic defor-

mation. Phase separation into FM and CE-AFM, like it has been discussed for LCMO with $0.4 \leq x \leq 0.5$ [8], can lead to the inhomogeneous magnetic and electric state of the cSL.

In summary we have shown that engineering of the doping profile in LCMO-BTO superlattices has massive influences on the magnetotransport properties and structure of the manganite layers. Only two monolayers of LMO at each interface lead to an enhancement of the

saturation magnetization. We discussed, that in conventional LCMO/BTO superlattices the ground state of the interfacial LCMO layers is likely CE-AFM, supporting theoretical calculations [19]. This phase is responsible for exceptional nonlinear (3ω) transport as well as for zfc-fc splitting of the linear resistance discussed within correlated polaron model and phase separation scenario. This work was supported by DFG via SFB 602, TPA2.

-
- [1] A. Ohtomo and H. Y. Hwang, *Nature* **427**(6973), 423 (Jan. 2004).
- [2] S. Thiel, G. Hammerl, A. Schmehl, C. W. Schneider, and J. Mannhart, *Science* **313**(5795), 1942 (2006).
- [3] E. Dagotto, *Physics* **2**, 12, 12 (Feb 2009).
- [4] N. Nakagawa, H. Y. Hwang, and D. A. Muller, *Nat Mater* **5**(3), 204 (Mar. 2006).
- [5] G. M. Muller, J. Walowski, M. Djordjevic, G.-X. Miao, A. Gupta, A. V. Ramos, K. Gehrke, V. Moshnyaga, K. Samwer, J. Schmalhorst, *et al.*, *Nat Mater* **8**(1), 56 (Jan. 2009).
- [6] B. Nadgorny, I. I. Mazin, M. Osofsky, R. J. Soulen, P. Broussard, R. M. Stroud, D. J. Singh, V. G. Harris, A. Arsenov, and Y. Mukovskii, *Phys. Rev. B* **63**(18), 184433 (Apr. 2001).
- [7] P. Schiffer, A. P. Ramirez, W. Bao, and S.-W. Cheong, *Phys. Rev. Lett.* **75**(18), 3336 (Oct. 1995).
- [8] J. van den Brink, G. Khaliullin, and D. Khomskii, *Phys. Rev. Lett.* **83**(24), 5118 (Dec 1999).
- [9] D. I. Khomskii, *International Journal of Modern Physics B* **15**, 2665 (2001).
- [10] G.-m. Zhao, V. Smolyaninova, W. Prellier, and H. Keller, *Phys. Rev. Lett.* **84**(26), 6086 (Jun. 2000).
- [11] A. S. Alexandrov and A. M. Bratkovsky, *Phys. Rev. Lett.* **82**(1), 141 (Jan. 1999).
- [12] C. P. Adams, J. W. Lynn, Y. M. Mukovskii, A. A. Arsenov, and D. A. Shulyatev, *Phys. Rev. Lett.* **85**(18), 3954 (Oct. 2000).
- [13] C. S. Nelson, M. v. Zimmermann, Y. J. Kim, J. P. Hill, D. Gibbs, V. Kiryukhin, T. Y. Koo, S.-W. Cheong, D. Casa, B. Keimer, *et al.*, *Phys. Rev. B* **64**(17), 174405 (Oct. 2001).
- [14] M. Bibes, S. Valencia, L. Balcells, B. Martínez, J. Fontcuberta, M. Wojcik, S. Nadolski, and E. Jedryka, *Phys. Rev. B* **66**(13), 134416 (Oct 2002).
- [15] M. Huijben, L. W. Martin, Y.-H. Chu, M. B. Holcomb, P. Yu, G. Rijnders, D. H. A. Blank, and R. Ramesh, *Physical Review B (Condensed Matter and Materials Physics)* **78**(9), 094413, 094413 (7 pages) (2008).
- [16] H. Yamada, Y. Ogawa, Y. Ishii, H. Sato, M. Kawasaki, H. Akoh, and Y. Tokura, *Science* **305**(5684), 646 (2004).
- [17] Y. Ishii, H. Yamada, H. Sato, H. Akoh, Y. Ogawa, M. Kawasaki, and Y. Tokura, *Applied Physics Letters* **89**(4), 042509, 042509 (3 pages) (2006).
- [18] F. Giesen, B. Damaschke, V. Moshnyaga, K. Samwer, and G. A. Müller, *Phys. Rev. B* **69**(1), 014421 (Jan 2004).
- [19] L. Brey, *Physical Review B (Condensed Matter and Materials Physics)* **75**(10), 104423, 104423 (7 pages) (2007).
- [20] I. Leonov, N. Binggeli, D. Korotin, V. I. Anisimov, N. Stojic, and D. Vollhardt, *Physical Review Letters* **101**(9), 096405, 096405 (4 pages) (2008).
- [21] V. Moshnyaga, K. Gehrke, O. I. Lebedev, L. Sudheendra, A. Belenchuk, S. Raabe, O. Shapoval, J. Verbeeck, G. V. Tendeloo, and K. Samwer, *Physical Review B (Condensed Matter and Materials Physics)* **79**(13), 134413, 134413 (8 pages) (2009).
- [22] V. Moshnyaga, I. Khoroshun, A. Sidorenko, P. Petrenko, A. Weidinger, M. Zeitler, B. Rauschenbach, R. Tidecks, and K. Samwer, *Applied Physics Letters* **74**(19), 2842 (1999).
- [23] I. K. Schuller, *Phys. Rev. Lett.* **44**(24), 1597 (Jun. 1980).
- [24] P. G. Radaelli, M. Marezio, H. Y. Hwang, S.-W. Cheong, and B. Batlogg, *Phys. Rev. B* **54**(13), 8992 (Oct. 1996).
- [25] M. J. Hÿtch and M. Gandais, *Philosophical Magazine A* **72**(3), 619 (1995).
- [26] G. Q. Gong, A. Gupta, G. Xiao, P. Lecoeur, and T. R. McGuire, *Phys. Rev. B* **54**(6), R3742 (Aug. 1996).
- [27] M.-H. Jo, N. D. Mathur, J. E. Evetts, M. G. Blamire, M. Bibes, and J. Fontcuberta, *Applied Physics Letters* **75**(23), 3689 (1999).
- [28] I. Gonzalez, S. Okamoto, S. Yunoki, A. Moreo, and E. Dagotto, *Journal of Physics: Condensed Matter* **20**(26), 264002 (7pp) (2008).
- [29] C. Adamo, C. A. Perroni, V. Cataudella, G. D. Filippis, P. Orgiani, and L. Maritato, *Physical Review B (Condensed Matter and Materials Physics)* **79**(4), 045125, 045125 (5 pages) (2009).
- [30] M. Yahia and H. Batis, *European Journal of Inorganic Chemistry* **2003**(13), 2486 (2003).